Supplemental material to

Kinetics of H_2O_2-driven degradation of chitin by a bacterial lytic polysaccharide monooxygenase

Silja Kuusk[†], Bastien Bissaro[§], Piret Kuusk[‡], Zarah Forsberg[§], Vincent G.H. Eijsink[§], Morten Sørlie[§], Priit Väljamäe[†1]

[†]Institute of Molecular and Cell Biology, University of Tartu, Estonia

[§]Faculty of Chemistry, Biotechnology and Food Science, Norwegian University of Life Sciences, Norway

[‡]Institute of Physics, University of Tartu, Estonia

Table S1. Kinetic parameters derived from time-curves of CBP21 reactions carried out with different AscA concentrations (Fig. 1A of the main article).

AscA (μM)	$[NAG_{eq}]_{max}$ (μM)	k^{obs} (s^{-1})	$k^{obs}[NAG_{eq}]_{max}$ (μM s^{-1})
10	78±1	0.0077±0.0004	0.60±0.03
100	84±3	0.0073±0.0004	0.61±0.03
1000	93±4	0.0078±0.0001	0.72±0.03

From Fig. 1A and Table S1 it follows that variation of the concentration of AscA over two orders of magnitude had no major effects on the kinetics of degradation of CNWs. In the experiments with 20 μM H_2O_2, 100 μM AscA and [CNWs] at 1.0 mg ml^{-1} or higher, $[NAG_{eq}]_{max}$ is determined by the amount of H_2O_2 with a stoichiometry of approximately 4 NAG_{eq} produced per one molecule of H_2O_2 (Fig. 3A and Fig. 4 of the main article). It is important to note that the experiments with different concentrations of AscA result in similar $[NAG_{eq}]_{max}$ values (Table S1). AscA may reduce H_2O_2, which would decrease the amount of H_2O_2 available for the CBP21 reaction. If the non-enzymatic consumption of H_2O_2 was significant, one would expect to see lower $[NAG_{eq}]_{max}$ values at higher AscA concentrations. Similar $[NAG_{eq}]_{max}$ values obtained at very different AscA concentrations, thus, indicate that non-enzymatic consumption of H_2O_2 in the reaction with AscA is not significant under our experimental conditions. In the conditions used here it appears that AscA played only the role of reducing the CBP21. Given the molar excess between AscA and CBP21 (between 200 and 20,000-fold excess) and the similarity of the three time-curves, the reduction was likely carried out with the same efficiency for the three different AscA concentrations.

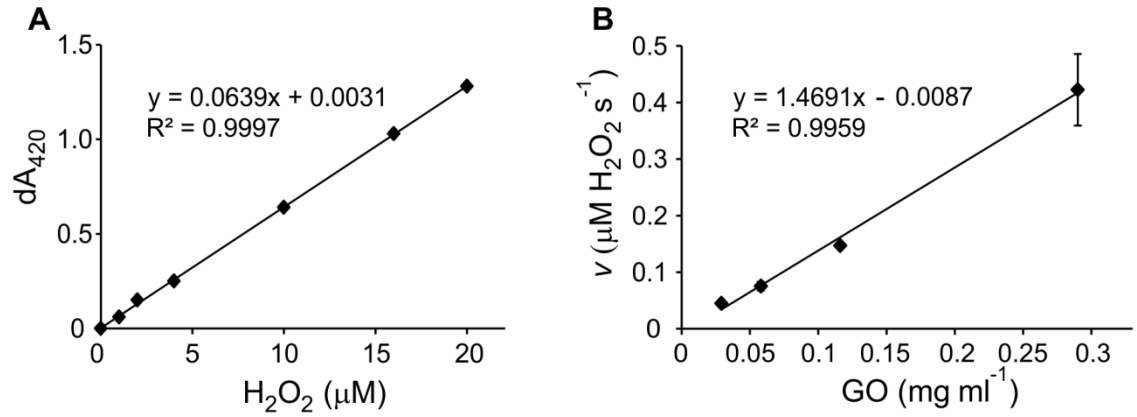

Figure S1. Calibration of the rate of formation of H_2O_2 in the glucose/glucose oxidase (GO) reaction. (A) H_2O_2 at different concentrations was incubated with 0.2 mM 2,2´-azino-bis(3-ethylbenzothiazoline-6-sulfonic acid) (ABTS) and horseradish peroxidase (HRP) in NaAc buffer (50 mM, pH = 6.1) at 25 ºC. The experiments were conducted in a spectrophotometer cuvette and the progress of the reaction was followed by recording the increase in absorbance at 420 nm over time. The concentration of HRP (15 U ml^{-1}) was selected so that the reactions were completed within the first minute. Linear regression of this standard curve gives a slope of 0.064 dA_{420}/μM H_2O_2 as conversion coefficient. (B) H_2O_2 formation rate as a function of GO concentration. Different concentrations of GO (0.025-0.3 mg ml^{-1}) were incubated in NaAc buffer (50 mM, pH = 6.1) at 25 ºC with ABTS (0.2 mM), HRP and glucose (10 mM). The production of H_2O_2 was followed by recording the increase in absorbance at 420 nm over time. The concentration of HRP (100 U ml^{-1}) was selected high enough so that the rate of the increase in the absorbance at 420 nm was independent of its concentration (ensuring thus that the rate measured is that of GO). With all GO concentrations, the increase in the absorbance at 420 nm over time was linear. The steady-state rates of H_2O_2 production (v_{H2O2}) were found from the slopes of the time curves and are plotted against GO concentration in panel B.

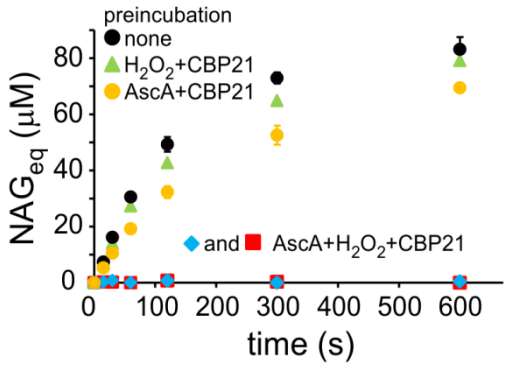

Figure S2. Inactivation kinetics of CBP21. Pre-incubations (for 10 min) in different conditions were followed by starting the LPMO reaction (see below) and monitoring of the formation of soluble products (in NAG equivalents) over 600 s. The pre-incubation conditions were:
None (black circles): no pre-incubation, i.e. a reference reaction performed with 1.0 mg ml^{-1} CNW, 20 µM H_2O_2, 0.1 mM ascorbic acid (AscA) and 50 nM CBP21.
H_2O_2 + CBP21 (green triangles): pre-incubation of 50 nM CBP21 with 20 µM H_2O_2; the reaction was started by the addition of a mixture of AscA and CNW to give a final concentrations of 0.1 mM and 1.0 mg ml^{-1}, respectively.
AscA + CBP21 (yellow circles): pre-incubation of 50 nM CBP21 with AscA (0.1 mM); the reaction was started by the addition of CNW (to 1.0 mg ml^{-1}) followed by H_2O_2 (to 20 µM)
AscA + H_2O_2 + CBP21 (red squares): pre-incubation of 50 nM CBP21 with 20 µM H_2O_2 and 0.1 mM AscA; the reaction was started by the addition of CNW (to 1.0 mg ml^{-1}). As an extra control another reaction was performed (blue diamonds) in which after the pre-treatment with AscA + H_2O_2 + CBP21 the mixtures were not only supplemented with CNW (to 1.0 mg ml^{-1}) but also with a fresh portion of AscA (to 0.1 mM) and H_2O_2 (to 20 µM), to compensate for potential depletion during the pre-incubation.

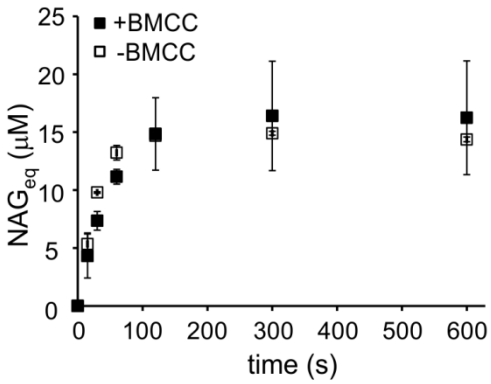

Figure S3. Degradation of CNWs by CBP21 in the presence and absence of bacterial microcrystalline cellulose (BMCC). Reactions contained CNWs (0.5 mg ml^{-1}), CBP21 (50 nM), H_2O_2 (100 μM), and AscA (0.1 mM). Reactions were conducted in NaAc (50 mM, pH 6.1) at 25 ºC in the presence (solid black squares) or absence (empty squares) of BMCC (2 mg ml^{-1}). Within error limits, the presence of BMCC had no effect on degradation of CNWs. This suggests that the relieved inactivation of CBP21 observed in the experiments with higher CNW concentrations is not caused by the protective effect of solid material in the reaction mixture.

Bacterial microcrystalline cellulose (BMCC) was prepared by HCl-hydrolysis of bacterial cellulose (*Gluconobacter xylinum*, ATCC 53582) as described in (Velleste et al 2010).

Velleste, R., Teugjas, H., and Väljamäe, P. (2010) Reducing end-specific fluorescence labeled celluloses for cellulase mode of action. *Cellulose* **17,** 125-138

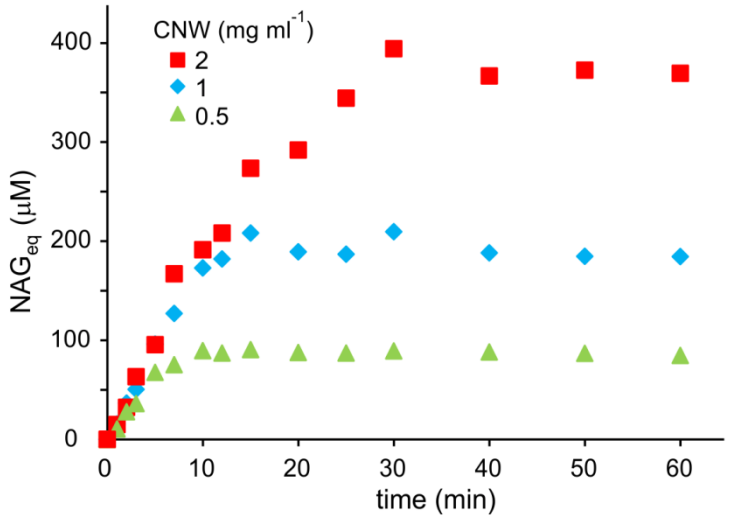

Figure S4. Formation of soluble products (in NAG equivalents, NAG_{eq}) during the degradation of CNWs by CBP21 fueled by the glucose/glucose oxidase (GO) system. The reactions contained CNWs (concentrations are given in the plot), CBP21 (50 nM), AscA (0.1 mM), glucose (10 mM) and GO (0.058 mg ml^{-1}, corresponding 0.075 µM $H_2O_2.s^{-1}$; see Fig. S1). For all CNW concentrations the rate of H_2O_2 production by the glucose/glucose oxidase system was lower than the apparent V_{max} of its consumption in a CBP21 reaction, which was 0.129 µM $H_2O_2.s^{-1}$ [calculated from an observed 0.52 NAG_{eq} s^{-1} (see Fig. 3D), which is divided by 4 (NAG_{eq}/H_2O_2)] for the lowest concentration of CNWs used (0.5 mg ml^{-1}). Reactions were conducted in NaAc buffer (50 mM, pH = 6.1) at 25 ºC. Reactions were started by the addition of GO to the mixture of CNWs, CBP21, AscA and glucose.

For all CNW concentrations the linear region of the formation of soluble products is followed by the abrupt decay of the rate. The leveling-off concentrations of soluble products were 88 µM, 190 µM, and 376 µM NAG equivalents for the experiments with CNW concentrations of 0.5 mg ml^{-1}, 1.0 mg ml^{-1}, and 2.0 mg ml^{-1}, respectively. Considering the total amount of NAG equivalents in CNWs (4.92 µmol/mg CNWs), these figures translate to an average degree of degradation of CNWs of 3.7 % ± 0.2 %. Rapid rate retardation already at low degrees of total degradation is often observed with enzymatic degradation of recalcitrant polysaccharides and a number of different factors have been proposed to be responsible for the phenomenon (Bansal et al 2009). Identification of the factors responsible for rapid rate retardation in CBP21 catalyzed degradation of CNWs at degrees of conversion above 3 % is beyond the scope of the present study. Within the scope of the present study, it is important to note that, in the phase preceding this degradation threshold, the formation of NAG_{eq} is essentially linear over time (provided that H_2O_2 is supplied at constant and low rates). In all concentration dependence experiments presented in this study, the degree of total degradation of CNWs remained well below the 3 % of total degradation of CNWs. For these reasons the concentration of CNWs can be taken as time invariant in Eq. 5.

Bansal, P., Hall, M., Realff, M.J., Lee, J.H., and Bommarius, A.S. (2009) Modeling cellulase kinetics on lignocellulosic substrates. *Biotechnol. Adv.* **27,** 833-848

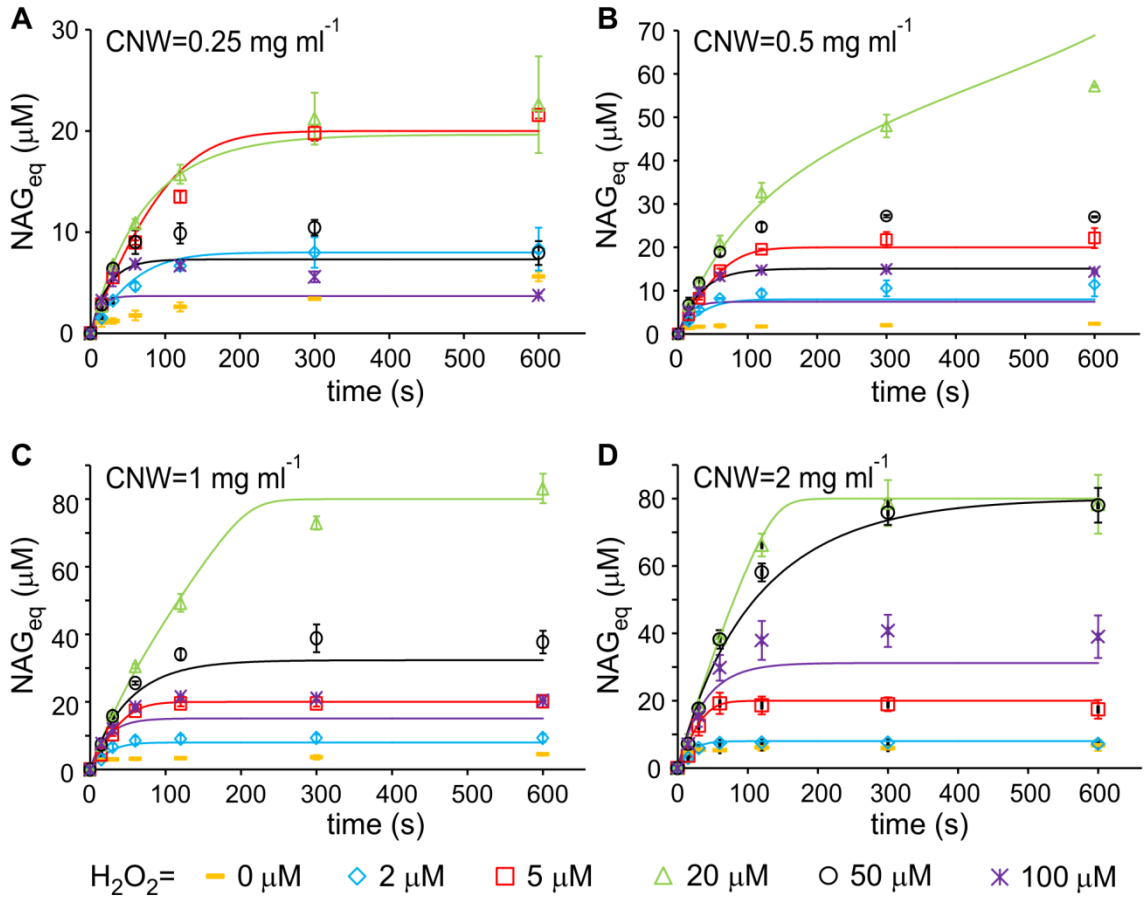

Figure S5. Impact of H_2O_2 and CNWs concentrations on the release of soluble products (in NAG equivalents) from CNWs by CBP21. The reaction mixtures contained CNWs, H_2O_2, CBP21 (50 nM) and AscA (0.1 mM). The readings of the experiments without the addition of H_2O_2 (H_2O_2 = 0 µM) were subtracted from the readings of the corresponding experiments with H_2O_2. The H_2O_2 dose-response experiments (see legend code in the figure) were done at four concentrations of CNWs: (A) 0.25, (B) 0.5, (C) 1.0 and (D) 2.0 mg ml^{-1}. All reactions were carried out in NaAc buffer (50 mM, pH 6.1) at 25 ºC and were initiated by addition of H_2O_2. Error bars show SD and are from at least two independent experiments. Solid lines represent the best-fit of global non-linear regression analysis of numerical solutions according to the combined Eqs. 4 and 5. The combined Eqs. 4 and 5 were applied to the whole dataset using 4th order Runge Kutta numerical integration in Microsoft Excel. The second order rate constant for inactivation of CBP21 in the absence of CNWs (k_i) was found by global non-linear regression analysis using Excel Solver. The values of all other parameters were obtained using different approaches described in the main manuscript (Fig. 8) and were fixed in the analyses. The fixed values were as follows: k_{cat} = 5.6 (H_2O_2 s^{-1}), n = 4 (NAG_{eq}/H_2O_2), $K_{i(CNW)}$ = 0.68 mg ml^{-1}, $K_{M(CNW)}$ = 0.58 mg ml^{-1}, $K_{M(H2O2)}$ = 2.8 µM. The best-estimate value of k_i was found to be 0.00128 μM^{-1} s^{-1}. Note that with some series there are significant deviations between experiment and the model. These are at least partly because of the stringent conditions used in the analysis, as only one parameter was let free when analyzing the whole dataset.

Analytical solutions for the limiting cases of eq 5 of the main article:

$$\frac{d[NAG_{eq}]}{dt} = \frac{[CNW][H_2O_2]_{(t)} n k_{cat}[CBP21]_{tot} e^{-k_i^{app}[H_2O_2]_{(t)}t}}{K_{i(CNW)}K_{M(H_2O_2)} + K_{M(H_2O_2)}[CNW] + K_{M(CNW)}[H_2O_2]_{(t)} + [CNW][H_2O_2]_{(t)}}$$

Equation 5 of the main article (shown above) has no analytical solution in the terms of elementary functions. Here, we analyze two limiting cases of Eq. 5. In the first case we use the approximation that the concentrations of both CNWs and H_2O_2 are time invariant. While the approximation that [CNW] is time invariant is plausible under our experimental conditions (Fig. S4), assuming the same for H_2O_2 is plausible only for the experiments with high concentrations of H_2O_2. Replacing time dependent $[H_2O_2]_{(t)}$ with time invariant initial concentration of $[H_2O_2]_0$ in Eq. 5 and solving for the product $[NAG_{eq}]$ results in Eq. S1.

$$[NAG_{eq}] = \frac{\frac{[CNW]}{K_{M(CNW)}} n k_{cat}[CBP21]_{tot}\left(1 - e^{-k_i^{app}[H_2O_2]_0 t}\right)}{k_i\left(\frac{K_{M(H_2O_2)}\left(K_{i(CNW)} + [CNW]\right)}{K_{M(CNW)} + [CNW]} + [H_2O_2]_0\right)} \quad \text{(S1)}$$

Note that the apparent second order rate constant for H_2O_2 inactivation of CBP21 (k_i^{app}) is defined in Eq. 4 of the main article. Provided with further assumptions that $K_{M(CNW)} \approx K_{i(CNW)}$ and $[H_2O_2]_0 >> K_{M(H2O2)}$ Eq. S1 reduces to Eq. S2.

$$[NAG_{eq}] = \frac{[CNW] n k_{cat}[CBP21]_{tot}}{K_{M(CNW)}[H_2O_2]_0 k_i}\left(1 - e^{-k_i^{app}[H_2O_2]_0 t}\right) \quad \text{(S2)}$$

Note that Eq. S2 is in the same form as Eq. 1 of the main article. Global non-linear regression analysis of time curves made with 50 μM and 100 μM concentrations (total 8 time-curves) of H_2O_2 according to Eq. S2 resulted in the value of second order rate constant for inactivation of CBP21 in the absence of CNWs (k_i) of 955 M^{-1} s^{-1}. The values of all other parameters (obtained using different approaches described in the main manuscript, Fig. 8) were fixed, as follows: k_{cat} = 5.6 (H_2O_2 s^{-1}), n = 4 (NAG_{eq}/H_2O_2), and $K_{M(CNW)}$ = 0.58 mg ml^{-1}. Note that using the whole dataset and global non-linear regression analysis of numerical solutions of Eqs. 4–5 (Fig. S5) resulted in the k_i estimate of 1280 M^{-1} s^{-1} (Fig. S5). Analysis of the dependency of k_i^{app} from the concentration of CNWs (Fig. 6) according to Eq. 4 of the main article results in the k_i estimate of 778 M^{-1} s^{-1}. Although different approaches result in somewhat different estimates for the value of k_i, they all fall in the order of 10^3 M^{-1} s^{-1}.

Next we analyzed Eq. 5 using the approximation that enzyme inactivation has negligible influence on the kinetics. In this case the exponential term can be omitted from Eq. 5. This approximation is plausible for the experiments with low concentrations of H_2O_2 and high concentrations of CNWs. With these premises in mind, the solving of Eq. 5 for the product $[NAG_{eq}]$ results in Eq. S3.

$$nK_{M(H_2O_2)}\left(K_{i(CNW)} + [CNW]\right)\ln\left(\frac{n[H_2O_2]_0}{n[H_2O_2]_0 - [NAG_{eq}]}\right) + \left(K_{M(CNW)} + [CNW]\right)[NAG_{eq}] = [CNW] n k_{cat}[CBP21]_{tot} t \quad \text{(S3)}$$

Eq. S3 has the form of as integrated Michaelis-Menten equation (Cornish-Bowden 1999). Assuming further that $K_{M(CNW)} \approx K_{i(CNW)}$, Eq. S3 reduces to Eq. S4.

$$\ln\left(\frac{n[H_2O_2]_0}{n[H_2O_2]_0 - [NAG_{eq}]}\right) + \frac{[NAG_{eq}]}{nK_{M(H_2O_2)}} = \frac{[CNW]k_{cat}[CBP21]_{tot}t}{K_{M(H_2O_2)}(K_{M(CNW)} + [CNW])}$$

(S4)

Provided that the initial concentration of H_2O_2 is low, the linear term on the left-hand side of Eq. S4 can be omitted (the maximum value of $[NAG_{eq}]$ equals $n[H_2O_2]_0$) and Eq. S4 reduces to Eq. S5.

$$[NAG_{eq}] = n[H_2O_2]_0\left(1 - e^{-\frac{k_{cat}[CBP21]_{tot}[CNW]}{K_{M(H_2O_2)}(K_{M(CNW)} + [CNW])}t}\right)$$

(S5)

Thus, it follows that at both limiting conditions, i.e. at high (Eq. S2) and at low (Eq. S5) H_2O_2 concentrations the time courses of NAG_{eq} product formation can be approximated by single exponential function in the form of Eq. 1 of the main article. However, the parameters of Eq. 1, $[NAG_{eq}]_{max}$ and k^{obs}, have different meanings depending on whether the kinetics is governed by enzyme inactivation (Eq. S2) or depletion of H_2O_2 (Eq. S5).

Cornish-Bowden A. Fundamentals of enzyme kinetics. 1999. London. U.K. Portland Press Ltd.